Original Article Clinics in Orthopedic Surgery 2023;15:725-733 • https://doi.org/10.4055/cios22392

Femoral Bowing Increases Early Postoperative Stress around the Femoral Stem in Humans: A Finite Element Analysis

Nobuhiro Kaku, MD, Tsuguaki Hosoyama, MD, Yutaro Shibuta, MD, Hiroshi Tsumura, MD

Department of Orthopaedic Surgery, Faculty of Medicine, Oita University, Yufu, Japan

Background: This study aimed to clarify the characteristics of stress distribution caused by the placement of tapered wedge stems in bowed femurs compared with that in normal femurs and the effect of varus stem placement.

Methods: Models with normal and enhanced bowing were created from the right-side computed tomography data of a 17-year-old woman with the least bowing among 40 participants who underwent anterior cruciate ligament reconstruction or operative treatment for trauma in our hospital between January 2017 and May 2018. Finite element analysis was performed, assuming the tapered wedge stem was placed in the neutral and varus positions.

Results: Varus stem placement on a femur with normal bowing showed a deviation and increase of von Mises stresses in the medial femur. Stem placement on a bowed femur, even when placed in the neutral position, increased stress across the periprosthetic bone. When the stem was placed in the varus position, von Mises stress across the periprosthetic bone increased. Zone 7, with strong bowing, demonstrated 3.6-fold increased stress compared with normal femurs. The maximum tensile principal stress was greatest in zone 6 and increased in zones 3 and 4.

Conclusions: Surgeons should assess femoral bowing preoperatively and pay particular attention to intraoperative stem alignment for femurs with high bowing.

Keywords: *Bowing, Femur, Finite element analysis, Stress, Stem*

Many high- and middle-income countries face an aging population,[1] which is associated with an increase in late-age-onset hip diseases, such as proximal femoral fractures.[2] This increase has in turn resulted in an increased frequency of bipolar hemiarthroplasty and total hip arthroplasty.[3] Recently, the use of cementless stems has become more common in older adults due to improved clinical outcomes.[4] One of the age-related changes reported in recent years is the enhancement of femoral bowing;[5,6] Oh et al.[7] reported an association between femoral shaft bowing deformity and atypical fractures occurring in the middle of the femur, while Matsumoto et al.[8] reported that the femur of Japanese individuals becomes more curved with age, which may contribute to the progression of medial-type knee osteoarthritis. These studies reported that the progressive trend towards femoral bowing with age contributes to the onset and progression of trauma and degenerative diseases.

Femoral bowing also influences treatment strategies. The insertion of intramedullary nails in bowed femur fractures requires relatively high surgical skills, as the position and length of the intramedullary nail must be considered.[9,10] Similar to intramedullary nails, femoral stems for artificial joints are also likely to be perforated during long stem insertions in the diaphysis. The medullary cavity becomes wider as osteoporosis progresses, especially in older

Received December 19, 2022; Revised April 5, 2023;
Accepted April 29, 2023
Correspondence to: Nobuhiro Kaku, MD
Department of Orthopaedic Surgery, Faculty of Medicine, Oita University, 1-1 Idaigaoka Hasama-machi, Yufu City, Oita 879-5593, Japan
Tel: +81-97-586-5872, Fax: +81-97-586-6647
E-mail: nobuhiro@oita-u.ac.jp

adults.[11,12] Therefore, the stem size is larger,[13] particularly when cementless conventional fit-and-fill stem designs are used. The stem length is correspondingly longer; thus, the stem tip is more likely to contact the lateral cortical bone of the femur. Therefore, tapered wedge-type stems, which have relatively short stem lengths and stable results, are often chosen, particularly when the entire femur is short.[14] However, tapered wedge stems are more likely to cause intraoperative and early postoperative fractures than stems with conventional fit-and-fill stem designs.[15] The implant design and instrumentation system, including the broaching device, should thus be considered for fracture prevention when using tapered wedge stems.[16]

In total hip arthroplasty, tapered wedge types are often placed in malalignment.[17] Misaligned stems are particularly likely to occur with less invasive approaches, such as smaller skin incisions.[18] While varus stem placement also increases postoperative thigh pain and subsidence,[17,19] its influence on long-term clinical outcomes remains controversial.[17,20] Femoral bowing in older adults is also expected to present with lower bone density and higher fracture risk.[21] In addition, femoral bowing may have a mechanical influence on the surrounding bone in arthroplasty stem placement; however, no reports have yet investigated the stress distribution of stem placement in a bowed femur. This study will therefore provide insights into the occurrence of intraoperative fractures, as well as the postoperative progression of stress shielding around the stem, and the risk of delayed fracture. In this simulation study with a design frequently used in prosthesis research, we investigated the stress distribution of tapered wedge stems in bowed femurs compared with that in normal femurs. Thus, this study aimed to clarify the characteristics of stress distribution caused by the placement of tapered wedge stems in bowed compared with that in normal femurs and the effect of varus stem placement.

METHODS

Ethics

This simulation study with level II evidence was approved by the Ethics Committee of Oita University (July 22, 2016; No. 1052) and was performed in accordance with the ethical standards of the 1964 Declaration of Helsinki and its later amendments. Patients provided written informed consent for participation in this study before surgery.

Analytical Model

Forty individuals who underwent anterior cruciate ligament reconstruction or operative treatment for trauma in our hospital between January 2017 and May 2018 and who had postoperative computed tomography (CT) images of the total femur were included. CT images from the iliac wing to the knee joint were acquired using a 320-section multidetector helical CT scanner (Aquilion ONE First Genesis, TSX–305A/1W; Canon Medical Systems Corp., Tochigi, Japan) with 1-mm slice thickness. Models with normal and enhanced bowing were created from the right-side CT data of a 17-year-old woman with the least bowing among participants. Seven slice planes were defined from the most distal axial reference plane of the femoral condyle to the proximal femur. Then, three points of the medullary canal center were acquired from the most distal plane 1, intermediate plane 4, and proximal plane 7. Based on these points, we calculated the radius of the three-dimensional (3D) curvature. The length of the functional axis of this patient was 361.7 mm, with femoral bowing of R = 2,432.8. A 3D bony femoral model was created from the CT image data of the subject using the 3D medical imaging software Mimics Version 21.0.0.406 (Materialise NV, Leuven, Belgium). For the normal model, the shape was observed using the patient data, while for the bowing model, the 3D bone model was imported into the 3D computer-aided design software SolidWorks 2020 (Dassault Systèmes SE, Vélizy-Villacoublay, France); the flex function was used to simulate bowing.

The degree of bowing was set to be comparable, with the patient demonstrating the greatest amount of femoral bowing among older adults with proximal femur fractures whose CT scans were taken approximately at the same time (R = 2,432.8 mm). A Bergman's coordinate system was constructed for each model[22] (Fig. 1), and Mimics was used to determine the stem size and placement. The femoral cementless stem was a Mizuho tapered wedge stem (Avansera; Mizuho Corp., Tokyo, Japan), and the size was selected to achieve the same preoperative leg length, as well as to fit the medial cortical bone (Standard No. 3, product No. 11-746-03; stem length: 104 mm, stem width: 8.2 mm, stem neck offset: 36 mm).

Two patterns of placement were set up: neutral and varus placement. The normal placement was a neutral position, with the stem axis aligned with the femoral bone axis, and the stem neck axis aligned with the femoral neck axis. The varus position was considered the position where the stem was inverted 5° from the normal placement with respect to the frontal image in the femoral coordinate system (Fig. 1). The four conditions were normal femur + neutral stem alignment (N–N), normal femur + varus stem alignment (N–V), bowed femur + neutral stem alignment (B–N), and bowed femur + varus stem align-

ment (B–V). The femoral anteversion angle of the normal femur was 11.11°, while that of the bowed femur was 6.24°. The anterior angles of each stem were N–N (25.1°), N–V (25.9°), B–N (24.3°), and B–V (25.1°), with reference to the line connecting the medial and lateral femoral condyles (Fig. 1).

Finite element models were created and analyzed using the bone model data for neutral and varus stem placement. The computer-aided engineering software Abaqus CAE 2018 (Dassault Systèmes Simulia Corp., Johnston, RI, USA) was used for creation and analysis. Stem placement in the neutral position on a normal bone model was defined as N–N, stem placement in the varus position on a normal bone model was defined as N–V, stem placement in the neutral position on a femur with enhanced bowing was defined as B–N, and stem placement in the varus position on a femur with enhanced bowing was defined as B–V. The condition settings in this study were set within the clinically likely range of stem alignment, and excessive conditions for stem alignment were avoided to achieve clinical realism. The femoral and stem models comprised four-node tetrahedral elements with an element size of approximately 2.0 mm; the number of elements and nodes for each model are shown in Table 1.

The finite element method (FEM) analysis also considered the influence of the surrounding soft tissue, based on the report of Heller et al.[23] The load constraint conditions for the femur were those assumed for walking (Table 2). The material properties of the finite element model are shown in Table 3, and the loads acting on the femur and stem are illustrated in Table 2 and Fig. 2. The distal femur was assumed to be fully constrained. After analysis, based on Gruen's zone, the volumes of interest (VOIs) for the femur model were placed in the area in contact with the internal and external sides of the stem (Fig. 3). Each VOI was divided into an anteroposterior and posterior plane, and the mean value of the generated stress in each zone was determined. The ratios of increase or decrease in mean von Mises stress and tensile stress in each zone were investigated for each condition considering the N–N values.

Regarding the contact conditions between the stem and femur, the stem-to-bone friction coefficient was set to $\mu = 0.4$, the inferior-bottom to $\mu = 0$, and the press fit (amount of intuitive interference) to 0.05 mm.[24] The model and material properties were a two-layer model with cancellous and cortical bone (cancellous: E = 1,000 MPa, $\nu = 0.3$; cortical: E = 15,000 MPa, $\nu = 0.28$), and a titanium-6 aluminum-4 vanadium stem (E = 119,000 MPa, $\nu = 0.3$). The load was increased linearly, and calculations were performed using the dynamic implicit method to calculate the von Mises stress and maximum tensile principal stress.[25]

We compared the four groups using the Kruskal-

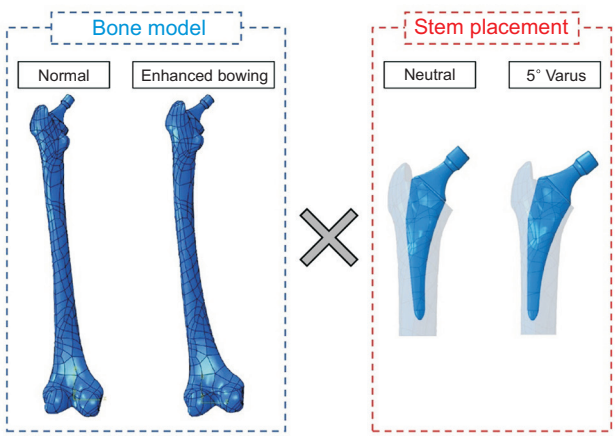

Fig. 1. *R*-values for normal femoral bowing (*R* = 2,432.8) and bowed femur (*R* = 1,528.0). The rotation was set to 5° from the normal placement with respect to the frontal image in the femoral coordinate system.

Table 1. Number of Elements for Each Condition and Its Model

Variable	Stem	Bone
Normal–neutral	47,447	501,910
Normal–varus	47,924	520,163
Bowel–neutral	47,902	500,544
Bowel–varus	47,924	511,152

Table 2. Material Properties (Linear Elastic Materials) Used in the Finite Element Simulations

Variable	Young's modulus (GPa)	Poisson's ratio
Cortical bone	15.0	0.28
Cancellous bone	1.0	0.3
Stem	113.0	0.3

Table 3. Load Acting on the Femur and Stem during Gait

Variable	X (N)	Y (N)	Z (N)
P0	–270.1	–164.0	–1,146.3
P1	32.4	7.6	40.4
P2	–0.5	9.3	–46.5

The three action points (P) of the attachments or wrapping points of the muscles are labeled P0, P1, and P2.

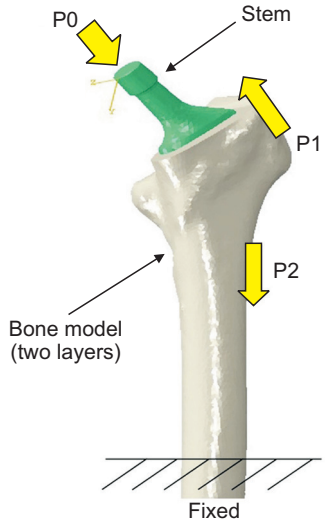

Fig. 2. Forces and constraints applied to the finite estimate (FE) models during walking. Loading conditions for the postoperative femoral FE model are based on the report by Heller et al.[23] using three action points (P) of the attachments or wrapping points of the muscles and labeled as P0 to P2.

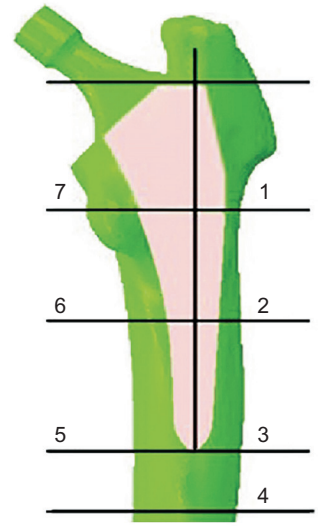

Fig. 3. Seven volumes of interest based on the Gruen zone. The bone around the stem was divided into seven three-dimensional sections based on Gruen's zone classification.

Wallis test and further used the Steel-Dwass method to compare between two groups. Comparisons were performed using EZR (version 1.5.1: Saitama Medical Center, Jichi Medical University, Japan), a graphical user interface of R (version 3.6.2; The R Foundation for Statistical Computing, Vienna, Austria), which is an improved version of the R commander (version 2.6-2), designed to incorporate statistical methods. After confirming significant differences between groups via the Kruskal-Wallis test, *p*-values were calculated by multiple comparisons using the Steel-Dwass method; *p*-values of ≤ 0.05 were considered significant.

RESULTS

In a normal bone model with less bowing, the von Mises stress significantly increased in all zones of the bone proximal to the medial stem in varus versus neutral stem placement, spreading to the anterior and posterior proximal femur (Table 4). The maximum tensile principal stress was observed in the varus stem placement, with a significant increase in stress observed in the calcar zone (Table 5). In the stem placement on the bowing femur, von Mises stresses in the distal medial part of the stem were significantly stronger than in the normal bone model, even in the neutral position; these stresses, as well as those in the proximal medial part of the stem, were even stronger when the stem was turned inward (Fig. 4). The maximum tensile principal stress significantly increased in the calcar area, as well as in the bone distal to the outer side of the stem (Fig. 5).

When comparing the N–N to the mean von Mises stress ratio of the models by zone, the von Mises stress of the bone corresponding with the medial side of the stem significantly increased with varus placement in the normal model in the anterior femur (Fig. 6A). However, for varus placement in normal bone, zones 2 and 3 showed a significant decrease. For the bowed femur, the stresses increased in the entire bone around the stem (even in the neutral placement, and even more in the varus placement), with the largest increase in mean stress being 3.64-fold higher anteriorly in zone 7A (B–V) and 2.92-fold higher posteriorly compared with N–N. In the posterior femur, the maximum stress in zone 7 was at N–V (Fig. 6B). With femoral bowing, the maximum tensile principal stress significantly increased in zones 6 and 7 anteriorly and in zones 3, 4, 6, and 7 posteriorly (Fig. 7).

DISCUSSION

In this study, varus stem placement in femurs with normal bowing demonstrated uneven and increased medial femoral stress in the medial part of the femur. Stem placement in a bowed femur caused an increase in periprosthetic bone stress when compared with a femur with standard bowing, even when placed in the neutral position. When the stem was placed in the varus position, the periprosthetic bone stress was found to increase further.

Table 4. Mean von Mises Stresses for the Four Conditions by Zone

Variable	1A	1P	2A	2P	3A	3P	4A	4P	5A	5P	6A	6P	7A	7P
N–N														
Mean	7.82	8.91	12.64	10.04	12.73	9.79	9.89	18.41	14.20	23.22	9.29	10.26	4.77	5.03
SD	5.37	6.59	7.06	7.39	3.21	4.53	6.39	9.75	7.31	4.42	3.74	5.10	2.21	2.02
N–V														
Mean	8.67	9.08	10.26	10.34	11.29	12.14	13.50	20.25	21.17	31.18	19.57	17.78	15.25	14.69
SD	6.21	5.88	7.11	5.77	5.04	6.11	8.86	11.09	10.11	5.33	7.14	8.83	9.16	9.06
B–N														
Mean	9.17	8.73	14.50	10.76	17.86	14.52	17.03	26.49	22.38	35.63	20.94	16.92	16.38	11.96
SD	6.34	4.06	8.08	5.75	5.08	6.89	9.69	12.94	11.18	7.54	6.69	9.05	9.42	7.50
B–V														
Mean	9.42	10.08	15.71	12.37	21.48	18.01	19.57	28.22	26.24	40.64	25.84	19.43	17.36	12.38
SD	6.31	6.03	7.66	7.27	7.31	8.78	10.64	13.98	13.51	9.12	9.84	11.85	11.22	9.44

All demonstrated significant differences in the comparison of each condition by zone.
A: anterior, P: posterior, N–N: normal–neutral, N–V: normal–varus, B–N: bowed–neutral, B–V: bowed–varus, SD: standard deviation.

Table 5. Average of the Maximum Tensile Principal Stresses by Zone for the Four Conditions

Variable	1A	1P	2A	2P	3A	3P	4A	4P	5A	5P	6A	6P	7A	7P
N–N														
Mean	7.52	8.05	12.32	9.97	13.15	9.62	7.33	4.99	3.43	-	2.64	2.51	3.35	3.92
SD	4.99	5.14	7.30	7.85	3.65	4.70	11.77	4.10	1.93	-	1.19	1.52	1.44	2.21
N–V														
Mean	8.40	8.40	10.48	9.95	12.09	11.02	9.38	6.58	1.81	-	18.22	11.23	15.26	14.74
SD	5.60	4.33	7.70	6.77	6.15	5.91	4.63	4.40	0.89	-	7.48	9.83	8.44	9.12
B–N														
Mean	8.78	8.63	13.32	10.81	18.22	15.68	14.63	13.91	6.45	-	19.02	9.61	15.94	12.24
SD	5.88	4.01	8.24	5.97	6.22	7.79	7.27	6.96	2.64	-	7.89	8.32	8.73	8.06
B–V														
Mean	8.91	9.46	14.88	12.69	22.10	20.12	17.75	17.25	6.95	-	21.49	10.86	17.50	13.13
SD	6.06	5.00	7.85	7.33	8.96	10.08	8.41	8.56	2.46	-	11.31	10.39	10.10	9.50

All demonstrated significant differences in the comparison of each condition by zone.
A: anterior, P: posterior, N–N: normal–neutral, N–V: normal–varus, B–N: bowed–neutral, B–V: bowed–varus, SD: standard deviation.

Several experimental reports regarding the changes in stress distribution due to inward stem placement have been previously published. Floerkemeier et al.[26] used a specially shaped Metha short stem (Aesculap AG, Tuttlingen, Germany) and performed mechanical tests with 10 strain gauges. They found that compared with lower osteotomies at the femoral neck, osteotomies at higher positions caused varus placement of the Metha stem. This

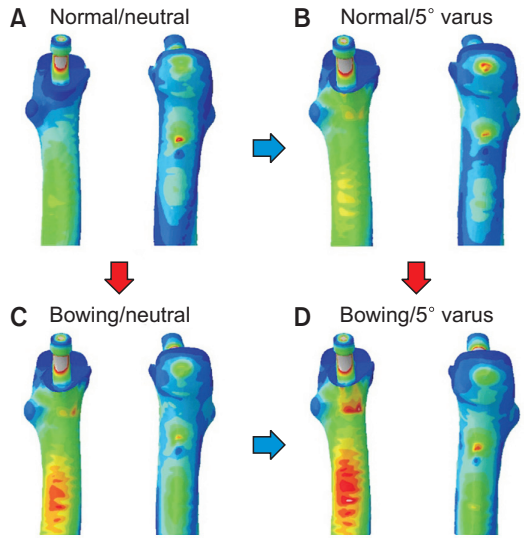

Fig. 4. Comparison of von Mises stresses in the four conditions. The figure shows the stem installation with a neutral position into the femur with normal bowing (A), 5° varus position into the femur with normal bowing (B), neutral position into the femur with severe bowing (C), and 5° varus position into the femur with severe bowing (D). Even in the normal femur, the medial femoral stresses corresponding with the medial side of the stem increased. The range of increase was extended when the stem was in the varus placement, and even neutral stem placement increased the medial femoral stresses due to the enhanced femoral bowing and was further placed in the varus placement.

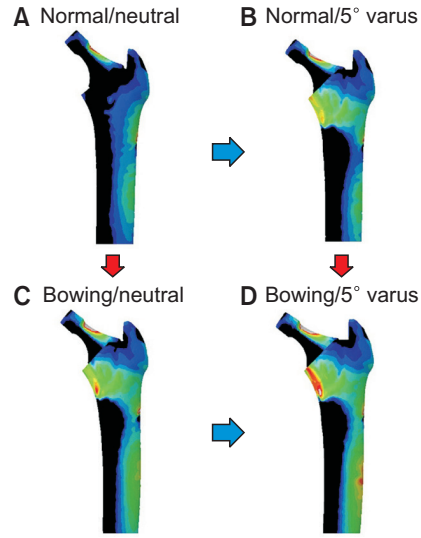

Fig. 5. Comparison of the maximum tensile principal stresses in four conditions. The figure shows the stem installation with a neutral position into the femur with normal bowing (A), 5° varus position into the femur with normal bowing (B), neutral position into the femur with severe bowing (C), and 5° varus position into the femur with severe bowing (D). In the varus placement on the bowing femur, there was an increase in stress in zones 4, 6, and 7. The red color in the distribution diagram represents higher tensile forces.

change in stem position resulted in an increased offset and consequently increased strain in the medial part of the proximal femur and near the distal end of the stem. Kwak et al.[27] performed a FEM analysis using an EcoFit stem (Implantcast, Buxtehude, Germany) with normal morphology. The authors demonstrated that even with a tapered wedge, varus insertion increased the micromotion around the stem, particularly given a short stem.

In this study, as shown in Table 4, uneven distribution of stresses occurred in femurs with normal bowing in areas where stresses decreased and increased with varus placement, with approximately three times the load observed in zone 7. The increased femoral offset increases the moment arm from the stem axis to the loading point because varus placement of the stem in a bowed femur further increases the femoral offset,[28,29] which might have increased the stress around the stem. The femur often has an inflection point near the center of the metaphysis and bows in an anterolateral direction.[5] Bowing of the femur results in a positional anomaly in the proximal femur, where the apex of the greater trochanter is elevated in relation to the center of the femoral head.[5] Thus, the femoral neck moves vertically with respect to the functional axis of the femur, and the diaphyseal center moves away from the functional axis. The actual anatomy of the proximal femur remains the same; however, the functional neck angle is reduced such that even if the stem is placed parallel to the proximal femoral medullary cavity, it is still placed in a varus position from the functional axis of the femur.

The difference in the ratio of the maximum tensile principal stress on the anterior and posterior femur (Fig. 7) was greatest in zone 6 (which is distal, beyond zone 7 in the calcar area) and increased in zones 3 and 4 (the distal outer area of the stem) due to increased femoral offset. One reason that the highest N–V stress was observed in posterior zone 7 is that stems with an equivalent anteversion angle would contact the cortical bone more anterior to the femoral neck osteotomy surface in bowed femurs (which have a lower femoral anteversion angle), and the stress on the bowed femur would be reduced on the opposite, posterior side. In addition, as fractures are more likely to occur in areas of tensile stress than in areas of compressive stress,[30] the possibility of fractures occurring in this area is high. However, in real-world clinical practice, fractures occur due to a complex combination of other factors, such as the patient's bone density, cortical thickness, and external loading; thus, a detailed study of individual fracture occurrence is desirable, with assessments considering

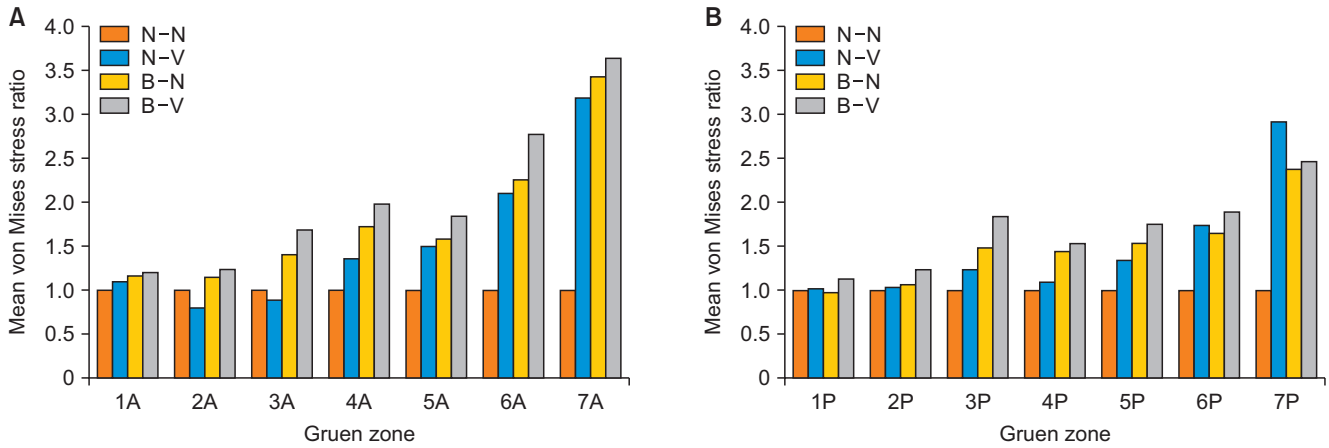

Fig. 6. Mean von Mises stress ratio (N–N vs. other) on the anterior (A) and posterior (B) femur. Except for zones 2 and 3, the stresses showed an increasing trend due to the varus placement and bone bowing. Zones 6 and 7 showed a large increase, with a maximum increase of approximately 3.64-fold. Conversely, the N–V stress was the highest in the rear zone 7. N–N: normal–neutral, N–V: normal–varus, B–N: bowed–neutral, B–V: bowed–varus, A: anterior, P: posterior.

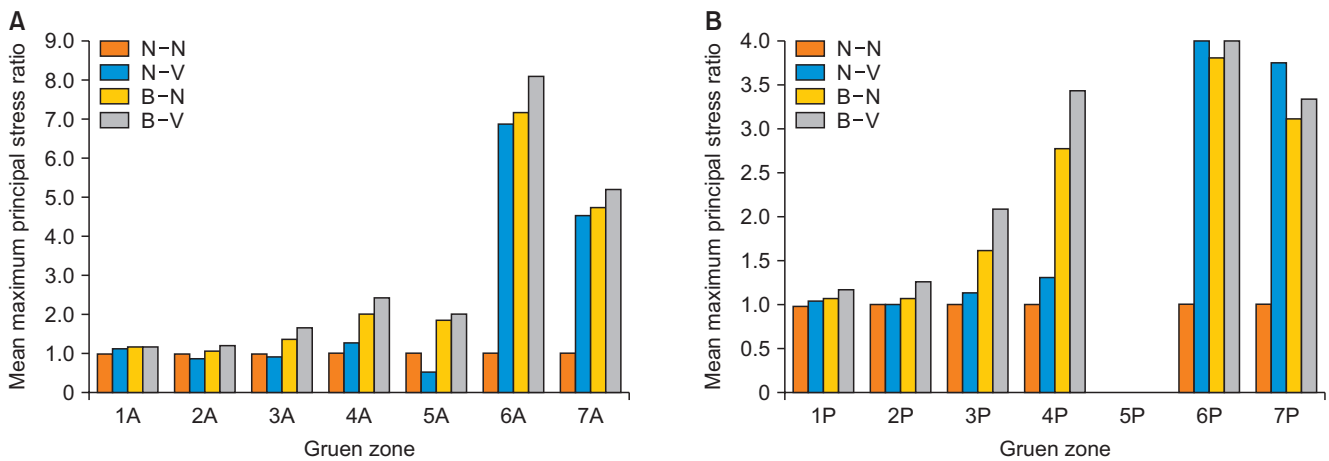

Fig. 7. Mean maximum tensile principal stress ratio (N–N vs. other) on the anterior (A) and posterior (B) femur. Anteriorly and posteriorly, the mean maximum tensile principal stress ratio was greatest in zone 6, with an increasing trend observed in zones 3 and 4 with femoral bowing and varus stem placement. By contrast, no tensile stress was found in the posterior zone 5. N–N: normal–neutral, N–V: normal–varus, B–N: bowed–neutral, B–V: bowed–varus, A: anterior, P: posterior.

individual physical properties.

A limitation of this study is that it does not cover complex clinical phenomena due to the uniformity of the set-up conditions, such as femoral length and thickness; degree of bowing; femoral osteotomy height; stem shape, size, and 3D installation angle; mechanical factors during walking; and load constraint condition involving only walking, but not standing. Local stress concentrations may occur when localized bone loss occurs, which cannot be reflected by a two-layer model that does not include detailed bone density information. However, in this study, the necessary conditions were set up to clarify the effect of the geometric change in femoral bowing on the stresses. Further studies with multifaceted conditions are required. While areas of high stress are more likely to result in fractures, these do not reflect fractures that occur in clinical practice.

In conclusion, when a stem is placed in a bowed femur, even in the neutral position, the stresses around the stem are unevenly distributed anteriorly and medially. In particular, a considerable increase in stress was observed in the calcar area compared to when the stem was placed in the normal femur. Moreover, with stem placement in a varus position, the stress increased further. Due to the increasing number of older patients, it is pertinent that surgeons should assess femoral bowing preoperatively.

Furthermore, it is also important for surgeons to accurately plan the stem alignment for femoral bowing to prevent complications due to inadequate stress distribution.

CONFLICT OF INTEREST

No potential conflict of interest relevant to this article was reported.

ACKNOWLEDGEMENTS

The authors thank Mizuho Corporation for preparing the commercial and noncommercial samples. Special thanks to Mr. Tsuchiya K, Mr. Yamada T, and Mr. Sanada A for their technical support in FEM analysis and many helpful discussions.

ORCID

Nobuhiro Kaku https://orcid.org/0000-0002-4041-1870
Tsuguaki Hosoyama https://orcid.org/0000-0002-8505-6534
Yutaro Shibuta https://orcid.org/0000-0001-5555-0905
Hiroshi Tsumura https://orcid.org/0000-0002-5384-822X

REFERENCES

1. Veras R. Population aging today: demands, challenges and innovations. Rev Saude Publica. 2009;43(3):548-54.
2. Miyasaka D, Endo N, Endo E, et al. Incidence of hip fracture in Niigata, Japan in 2004 and 2010 and the long-term trends from 1985 to 2010. J Bone Miner Metab. 2016;34(1):92-8.
3. Lee K, Goodman SB. Current state and future of joint replacements in the hip and knee. Expert Rev Med Devices. 2008;5(3):383-93.
4. Kim YH, Jang YS. Long-term clinical and radiographic results of an ultra-short metaphyseal-fitting non-anatomic cementless stem in patients with femoral neck fracture. J Arthroplasty. 2021;36(6):2105-9.
5. Tagomori H, Kaku N, Shimada T, Tsumura H. Effect of age and sex on femoral curvature in the Japanese population: three-dimensional computed tomography findings. Anat Sci Int. 2021;96(3):411-21.
6. Jung IJ, Choi EJ, Lee BG, Kim JW. Population-based, three-dimensional analysis of age- and sex-related femur shaft geometry differences. Osteoporos Int. 2021;32(8):1631-8.
7. Oh Y, Wakabayashi Y, Kurosa Y, Fujita K, Okawa A. Potential pathogenic mechanism for stress fractures of the bowed femoral shaft in the elderly: mechanical analysis by the CT-based finite element method. Injury. 2014;45(11):1764-71.
8. Matsumoto T, Hashimura M, Takayama K, et al. A radiographic analysis of alignment of the lower extremities: initiation and progression of varus-type knee osteoarthritis. Osteoarthritis Cartilage. 2015;23(2):217-23.
9. Harper MC, Carson WL. Curvature of the femur and the proximal entry point for an intramedullary rod. Clin Orthop Relat Res. 1987;(220):155-61.
10. Arnone JC, Crist BD, Ward CV, El-Gizawy AS, Pashuck T, Della Rocca GJ. Variability of human femoral geometry and its implications on nail design. Injury. 2021;52(1):109-16.
11. Takeuchi S, Kageyama I, Awatake T, Kato S, Yamashita H. Enlargement of the femoral marrow cavity with aging. Kaibogaku Zasshi. 1998;73(3):259-64.
12. Dorr LD, Faugere MC, Mackel AM, Gruen TA, Bognar B, Malluche HH. Structural and cellular assessment of bone quality of proximal femur. Bone. 1993;14(3):231-42.
13. Nishino T, Mishima H, Miyakawa S, Kawamura H, Ochiai N. Midterm results of the Synergy cementless tapered stem: stress shielding and bone quality. J Orthop Sci. 2008;13(6):498-503.
14. Ikemura S, Motomura G, Hamai S, et al. Tapered wedge stems decrease early postoperative subsidence following cementless total hip arthroplasty in Dorr type C femurs compared to fit-and-fill stems. J Orthop Surg Res. 2022;17(1):223.
15. Sershon RA, McDonald JF 3rd, Ho H, Hamilton WG. Periprosthetic femur fracture risk: influenced by stem choice, not surgical approach. J Arthroplasty. 2021;36(7S):S363-6.
16. Fleischman AN, Schubert MM, Restrepo C, Chen AF, Rothman RH. Reduced incidence of intraoperative femur fracture with a second-generation tapered wedge stem. J Arthroplasty. 2017;32(11):3457-61.
17. Khalily C, Lester DK. Results of a tapered cementless femoral stem implanted in varus. J Arthroplasty. 2002;17(4):463-6.
18. Teet JS, Skinner HB, Khoury L. The effect of the "mini" incision in total hip arthroplasty on component position. J Arthroplasty. 2006;21(4):503-7.
19. de Beer J, McKenzie S, Hubmann M, Petruccelli D, Winemaker M. Influence of cementless femoral stems inserted in varus on functional outcome in primary total hip arthro-

plasty. Can J Surg. 2006;49(6):407-11.

20. Coulomb R, Laborde A, Haignere V, Bauzou F, Marchand P, Kouyoumdjian P. Varus stem positioning does not affect long-term functional outcome in cementless anatomical total hip arthroplasty. Arch Orthop Trauma Surg. 2023;143(1):511-8.
21. Tsuchie H, Miyakoshi N, Kasukawa Y, et al. Factors related to curved femur in elderly Japanese women. Ups J Med Sci. 2016;121(3):170-3.
22. Bergmann G, Siraky J, Rohlmann A, Koelbel R. A comparison of hip joint forces in sheep, dog and man. J Biomech. 1984;17(12):907-21.
23. Heller MO, Bergmann G, Kassi JP, Claes L, Haas NP, Duda GN. Determination of muscle loading at the hip joint for use in pre-clinical testing. J Biomech. 2005;38(5):1155-63.
24. Biemond JE, Aquarius R, Verdonschot N, Buma P. Frictional and bone ingrowth properties of engineered surface topographies produced by electron beam technology. Arch Orthop Trauma Surg. 2011;131(5):711-8.
25. Bergmann G, Deuretzbacher G, Heller M, et al. Hip contact forces and gait patterns from routine activities. J Biomech. 2001;34(7):859-71.
26. Floerkemeier T, Gronewold J, Berner S, et al. The influence of resection height on proximal femoral strain patterns after Metha short stem hip arthroplasty: an experimental study on composite femora. Int Orthop. 2013;37(3):369-77.
27. Kwak DK, Bang SH, Lee SJ, Park JH, Yoo JH. Effect of stem position and length on bone-stem constructs after cementless hip arthroplasty. Bone Joint Res. 2021;10(4):250-8.
28. Hattori Y, Asai N, Mori S, et al. Femoral valgus correction angle for the intramedullary alignment rod is strongly associated with femoral lateral bowing in Japanese patients with varus knee osteoarthritis undergoing total knee arthroplasty. Adv Orthop. 2022;2022:7223534.
29. Xu J, Pierrepont J, Madurawe C, Shimmin A, Bruce W. The effect of varus stem placement on joint offset during total hip arthroplasty: a virtual study. Hip Int. 2022;32(5):620-6.
30. Saha S, Hayes WC. Relations between tensile impact properties and microstructure of compact bone. Calcif Tissue Res. 1977;24(1):65-72.